

1 Biophysical Reviews and Letters, Vol. 1, No. 3 (2006) 1–7  
 © World Scientific Publishing Company



3 **ELECTRICAL IMPEDANCE SPECTROSCOPY**  
 4 **CHARACTERIZATIONS OF ALKYL-FUNCTIONALIZED**  
 5 **SILICON(111)**

7 ELICIA L. S. WONG

8 *Biophysics and Bioengineering, School of Chemical and*  
 9 *Biomolecular Engineering, University of Sydney, NSW 2008, Australia*  
 10 *Australian Nuclear Science and Technology Organisation*  
 11 *Lucas Heights Research Laboratory, Lucas Height*  
*NSW 2234, Australia*  
*ew@ansto.gov.au*

13 TERRY C. CHILCOTT

14 *Biophysics and Bioengineering, School of Chemical and*  
 15 *Biomolecular Engineering, University of Sydney, NSW 2008, Australia*  
 16 *Seconded from School of Physics, University of New South Wales*  
 17 *NSW 2052, Australia*  
*tchilcot@chem.eng.usyd.edu.au*

19 MICHAEL JAMES

20 *Australian Nuclear Science and Technology Organisation*  
 21 *Lucas Heights Research Laboratory, Lucas Height, NSW 2234, Australia*  
*mja@ansto.gov.au*

23 HANS G. L. COSTER

24 *Biophysics and Bioengineering, School of Chemical and*  
 25 *Biomolecular Engineering, University of Sydney, NSW 2008, Australia*  
*hcoster@usyd.edu.au*

27 Received  
 Revised

29 This organic thin-film systems that are based on silicon-carbon covalent bonds have been  
 30 shown to lead to densely packed alkyl monolayers that have potential bio-passivation  
 31 or bio-sensing applications. Presented are electrical impedance spectroscopy (EIS) char-  
 32 acterisations of a series of alkyl monolayers  $[\text{CH}_3(\text{CH}_2)_m\text{CH}=\text{CH}_2; m = 7, 9, 11, 13, 15]$   
 33 that were covalently linked to Si(111) wafers. The characterizations reveal capacitance,  
 34 conductance and geometrical properties of the monolayers. The capacitance properties  
 35 yield estimates of thicknesses for the monolayers that increase proportionally with each  
 36 additional  $\text{CH}_2$  unit and are consistent with the known physical properties of these  
 37 films such as dielectric constants and chain canting angles. This study illustrates that  
 EIS characterizations are able to probe immobilized surfaces on silicon with sub-atomic

2 *E. L. S. Wong et al.*

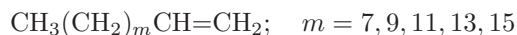
1 resolution which is so important in the development of practical bio-passivation or bio-sensing applications.

3 *Keywords:* Electrical impedance spectroscopy; self-assembled monolayer; thin film.

## 1. Introduction

5 The formation of self-assembled monolayer (SAMs) utilizing either the thiol-gold or organosilanes-silica chemistry have illustrated the powerful approach of harnessing  
7 “self-assembly” in the production of novel nanoscale biomolecular architectures on electronic solid surfaces. To gain a greater insight into the strategies for controlling  
9 the self assembly of the monolayers (SAMs), their bio-functionalization and the interfacing of the biological event with the electronic substrate, a detailed under-  
11 standing of the structure, molecular packing, surface termination and electrical storage, and conduction properties of SAMs are required. X-ray photoelectron spec-  
13 troscopy (XPS),<sup>1</sup> ellipsometry,<sup>2</sup> transmission electron microscopy (TEM),<sup>3</sup> atomic force microscopy (AFM)<sup>4,5</sup> and scanning tunneling microscopy (STM)<sup>6,7</sup> have pro-  
15 vided excellent bases for furthering the knowledge of the structure, order and bond-  
17 ing of SAMs. However, these techniques are either destructive or disruptive of the fundamental chemistries taking place at the bio-substrate interface that constitute  
19 the crucially important sensing (e.g. biorecognition) processes. Further, these tech-  
21 niques only probe the chemistry across a very small area (a few nm<sup>2</sup> or μm<sup>2</sup>) and sometimes only the surface of that area, which might not be a true representa-  
23 tion of the chemistry taking place over the whole surface and within the modified substrate.

23 The Electrical impedance spectroscopy (EIS) is a non-destructive and non-  
25 disruptive technique, that has proven effective in monitoring biological function and ultra structure *in vivo*.<sup>8</sup> Described herein is its use in characterizing a series of  
27 alkyl monolayers covalently bonded to the surface of highly doped Si(111) wafers in contact with an electrolyte. The formulas for the series are given by



29 which henceforth will be denoted by the notation  $C_n$  (i.e. C10, C12, C14, C16 and C18, respectively) where  $n$  denotes the total number of carbon atoms comprising  
31 the alkane. These characterizations illustrate the potential of EIS studies to elucidate the origin of electrical conduction in these layers.

## 33 2. Experimental Procedure

### 35 2.1. Materials

35 Reagent grade 1-decene, 1-dodecene, 1-tetradecene, 1-hexadecene, 1-octadecene, potassium chloride, hexane, tetrahydrofuran, dichloromethane, and methanol were  
37 purchased from Aldrich Chemicals (Sydney, NSW, Australia). Hydrogen peroxide, concentrated sulphuric acid, and absolute ethanol were purchased from Ajax

1 (Sydney, Australia). 40% ammonium fluoride was obtained from Kanto Kagaku  
 2 Singapore Pte Ltd. (Singapore). All the chemicals were used as received without  
 3 further purification. Milli-Q (18 M $\Omega$  cm) was used for the rinsing and preparation  
 of solutions.

## 5 **2.2. Preparation of Si-C linked monolayers**

6 Highly doped Si(111) wafer pieces (*n*-type, 0.01–0.1  $\Omega$ cm) were cleaned, etched in  
 7 ammonium fluoride solution and functionalized by hydrosilylation *via* thermal acti-  
 8 vation in neat alkene solution. The freshly etched Si(111)-H wafer was then added  
 9 to neat *n*-alkene (liquid) contained in a Schlenk flask that was heated in an oil  
 10 bath under vacuum. After cooling the functionalized silicon wafer was rinsed with  
 11 hexane, dichloromethane, tetrahydrofuran, and ethanol and dried thoroughly under  
 a stream of nitrogen.

## 13 **2.3. EIS measurements and analysis**

14 Gallium–indium eutectic was applied to surface of one side of the silicon wafer. The  
 15 wafer was placed on a metal plate with the gallium–indium eutectic face forming  
 an electrical contact of very low electrical resistance with the plate. An O-ring  
 17 of area  $1.81 \times 10^{-5} \text{ m}^2$  was then placed on the functionalized surface and held in  
 place by a sealed chamber into which a 33.3 mM potassium chloride electrolyte  
 19 was perfused. The chamber also supported platinum and Ag|AgCl electrodes that  
 were immersed in the electrolyte and served as a reference and counter electrodes  
 21 for the impedance measurements. The functionalized silicon wafer served as the  
 working electrode for the impedance measurements which were performed using a  
 23 high precision low frequency impedance spectrometer (INPHAZE Pty Ltd). This  
 impedance spectrometer<sup>9</sup> has particularly good phase angle resolution which allows  
 25 very precise determination of the capacitance (as well as the conductance) of the  
 alkane films.

27 The contributions to the measured impedance derive from the electrolyte and  
 monolayer whose bulk electrical properties are commonly modeled as Maxwell–  
 29 Wagner elements comprised of a single conductance component  $g$  representing the  
 electrolyte and a single capacitance component  $c_n$  representing the monolayer. This  
 31 assumes that the conductance of the alkane monolayer is very small compared with  
 the admittance of the capacitance element over the frequency range of interest. The  
 33 total impedance of the system is then given by

$$Z_T = \frac{1}{g} + \frac{1}{j\omega c_n}, \quad (1)$$

35 where  $\omega$  is the angular frequency of the AC current used for the impedance mea-  
 surements and  $j \equiv \sqrt{-1}$ . The electrically equivalent circuit for this model is shown

4 *E. L. S. Wong et al.*

1 in Fig. 1. The dependence of the impedance on frequency provides a means of dis-  
 2 tinguishing between these contributions. For example, the total capacitance and its  
 3 limiting value at low frequencies are given by

$$c_T(\omega) \equiv \text{Im} \left[ \frac{1}{Z_T} \right] \frac{1}{\omega} \approx c_n \quad \text{and} \quad c_T(\omega \rightarrow 0) \approx c_n \quad (2)$$

5 respectively. And the total conductance and its limiting value at high frequencies  
 6 are given by

$$g_T(\omega) \equiv \text{Re} \left[ \frac{1}{Z_T} \right] \quad \text{and} \quad g_T(\omega \rightarrow \infty) \approx g \quad (3)$$

7 respectively. The former yields the thickness,  $t$ , of the monolayers which is given by

$$t_n = \frac{\varepsilon_l \varepsilon_0}{c_n}, \quad (4)$$

9 where  $\varepsilon_l$  is the dielectric constant of the organic layer ( $= 2.05$ , which is the accepted  
 11 range for alkanes<sup>10</sup>) and  $\varepsilon_0$  is the permittivity of free space ( $= 8.85 \times 10^{-12}$  F).  
 12 The conductance element representing the electrolyte yields the distance  $d$  of the  
 13 reference electrode from the surface of the alkyl layer which is given by

$$d = \frac{\sigma}{g}, \quad (5)$$

15 where  $\sigma$  is known conductivity of the electrolyte. In these experiments every attempt  
 16 was made to locate the reference electrode in the same position for each alkyl layer,  
 17 i.e. to maintain  $d$  constant.

### 3. Results and Discussion

19 Figure 1 shows the impedance spectra obtained for the series of alkyl monolayers on  
 20 silicon. The spectra are expressed as dispersions of the conductance and capacitance  
 21 with frequency in order to distinguish between the contributions arising from the  
 22 monolayers and electrolyte that are given by Eqs. (2) and (3), respectively, which  
 23 derive from Eq. (1). The curves in Fig. 1 are the theoretical dispersions of con-  
 24 ductance and capacitance with frequency generated by Eq. (1) that were fitted to  
 25 the impedance spectra. The theoretical dispersions can be seen to predict generally  
 26 the observed dispersions over the whole frequency range and for all chain lengths  
 27 of the alkyls (i.e. all  $n$ ). The predictions are very precise for the conductance at  
 28 high frequencies and for the capacitance at low frequencies, where the dispersions  
 29 plateau to values which are independent of frequency yielding in the first instance,  
 30 an estimate of the capacitance of the monolayers  $c_n$ , and in the second, an estimate  
 31 of the conductance  $g$  of the electrolyte.

32 The estimated values for  $g$  were consistent with the known conductivity of a  
 33 100 mM KCl electrolyte and the distance  $d$  of the reference electrode from the  
 34 electrolyte/monolayer surface as described by Eq. (5). The variation in these values  
 35 was attributed to variations in  $d$  as a consequence of the unavoidable displacement  
 of the position of the electrode when changing silicon wafers.

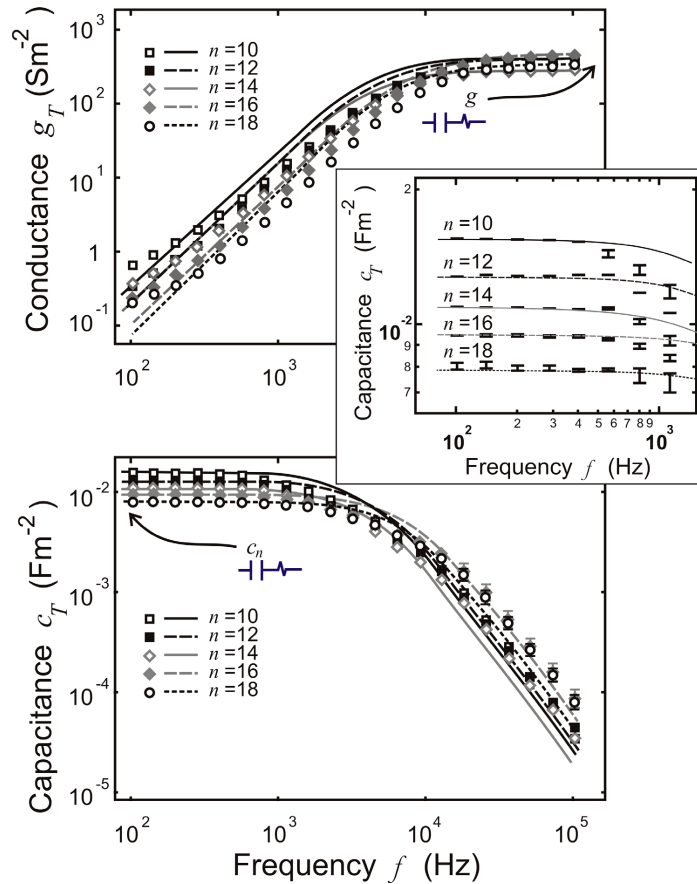


Fig. 1. Dispersions of the conductance and capacitance with frequency  $f$  ( $= \omega/2\pi$ ) for Si-C linked monolayers of alkyl chain lengths denoted by  $n$ . In most instances the symbols representing the data are larger than the standard deviations. The inset is an expansion of the scale of the capacitance data at low frequencies in which the symbols are not shown to illustrate that the standard deviations increase with increasing  $n$ . The curves represent the fits of the Maxwell-Wagner model given by Eq. (1) to these spectra.

1        Figure 1 shows that the capacitance at low frequencies decreases with increasing  
 2        chain length  $n$ , which is consistent with trends reported by Yu *et al.*<sup>11</sup> for chain  
 3        lengths of  $n = 2, 6, 10$ , and  $15$  for monolayers in contact with  $0.1 \text{ M H}_2\text{SO}_4 + 2\%$   
 4        HF and interfacial capacitive measurement obtained for alkanethiol monolayers on  
 5        gold.<sup>12,13</sup> Equation (2) shows that capacitance measurements, this frequency range  
 6        reflect those properties of the monolayers, i.e.  $c_n$  in Eq. (1), values for which can  
 7        be substituted into Eq. (4) to yield estimates of the thicknesses of the monolayers.  
 8        The inset to Fig. 1 shows the capacitance plots on a greatly expanded scale  
 9        and reveal that the standard deviations for the capacitance measurements in this  
 10        frequency range are very small and hence also the standard deviations for the esti-  
 11        mates of thicknesses will be very small. This is reflected in the plots of calculated

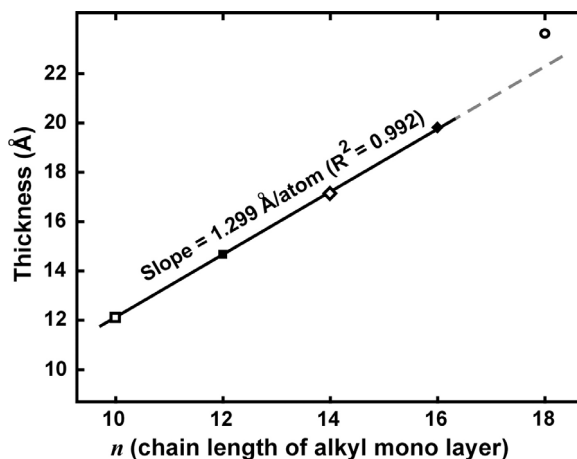
6 *E. L. S. Wong et al.*

Fig. 2. Thicknesses of the alkyl monolayers estimated from EIS data as a function of alkyl chain length  $n$ . Estimates were obtained using Eq. (4) and capacitance values for  $c_n$  obtained from fitting Eq. (1) to the EIS spectra shown in Fig. 1. The line reveals a strong linear correlation between thickness  $t_n$  and  $n$  for  $n = 10$  to 16. A larger increase in thickness  $t_n$  is seen for a further increase in the chain length to 18.

1 thicknesses of the alkyl layers as a function of  $n$ . This is shown in Fig. 2, where  
 2 the symbols representing the estimates are larger than the standards deviations for  
 3 these estimates.

4 Estimates of the thickness can be seen in Fig. 2 to increase with increasing  
 5 chain length  $n$ . The trend is highly linear for  $n = 10, 12, 14,$  and  $16$  ( $1.299 \text{ \AA}/\text{atom}$   
 6 with correlation coefficient of  $0.992$ ) but does not extend to the alkyl monolayer  
 7 of longest chain length (i.e.  $n = 18$ ). Further, the inset in Fig. 1 shows that the  
 8 standard deviations of the capacitance measurements, which form the bases of the  
 9 estimates of thicknesses, increased with increasing chain length. This suggests that  
 10 the thickness of an alkyl layer is more variable over time and the degree of the  
 11 variation, became more pronounced with increasing chain length  $n$  and was most  
 12 pronounced for  $n = 18$ . The variations in thickness with time and the larger than  
 13 expected thickness for the alkyl layer of chain length 18 may be the result of vari-  
 14 ations in the canting angle, i.e. the inclination of the alkyl molecules with respect  
 15 to the surface normal.<sup>14,15</sup>

16 Estimates of the canting angles were  $37.9^\circ, 36.5^\circ, 36.0^\circ, 35.5^\circ$  and  $30^\circ$  for  $n =$   
 17  $10, 12, 14, 16,$  and  $18,$  respectively, which are in good agreement with other reported  
 18 values for alkyl monolayers on Si(111) and Si(100) surfaces (e.g. Linford *et al.*<sup>16</sup>)  
 19 and analogous chain length of thiols on gold.<sup>17</sup> Theoretical calculations also indicate  
 20 that a  $\sim 30^\circ - 38^\circ$  canting angles on gold minimizes the energy for these surfaces.<sup>18</sup>

21 The EIS data yielded estimates of the canting angle that decreased with increas-  
 22 ing  $n$ . The trend was highly linear for  $n \leq 16$  as per the dependence of estimates  
 23 of the thickness on  $n$  shown in Fig. 2. Though the canting angle estimated for  
 24  $n = 18$  was consistent with the general trend it departed significantly from the  
 25 linear relationship established for shorter chain lengths.

#### 4. Conclusion

EIS characterizations of  $n$ -alkyl mono layers ( $n = 10, 12, 14, 16$ , and 18) functionalized on Si(111) surfaces have yielded estimates of the thicknesses of these layers that increased with increasing chain length. The standard deviations for the estimates of thickness, though generally less than an Å, also increased with increasing chain length. In contrast the canting angle of the alkyl molecules forming the layers decreased with increasing chain length. All of these trends were highly linear for  $n \leq 16$  the exception being the monolayer of chain length 18. Future studies will focus on exploring the lower frequency regimes of EIS with the view of characterizing the conduction properties of alkyl monolayers and elucidating the conduction mechanisms.

#### Acknowledgment

We would like to thank Australian Research Council (ARC) for the funding of this research (Discovery Grant Number: DP0452447).

#### References

1. D. A. Hutt and G. J. Leggett, *Langmuir* **13**, 3055 (1997).
2. A. N. Parikh, B. Liedberg, S. V. Atre, M. Ho and D. L. Allara, *J. Phys. Chem.* **99**, 9996 (1995).
3. L. Strong and G. M. Whitesides, *Langmuir* **4**, 546 (1988).
4. J. Pan, N. Tao and S. M. Lindsay, *Langmuir* **9**, 1556 (1993).
5. H. I. Kim, T. Koini, T. R. Lee and S. S. Perry, *Langmuir* **13**, 7192 (1997).
6. G. E. Poirier, *Chem. Rev.* **97**, 1117 (1997).
7. G. E. Poirier and M. J. Tarlov, *Langmuir* **10**, 2853 (1994).
8. T. C. Chilcott and H. G. L. Coster, *Annals of the New York Academy of Sciences* **873**, 269 (1999).
9. H. G. L. Coster, T. C. Chilcott and A. C. F. Coster, *Bioelectrochemistry and Bioenergetics* **40**, 79 (1996).
10. V. L. Lanza and D. B. Herrmann, *J. Polym. Sci.* **28**, 622 (1958).
11. H. Z. Yu, S. Morin, D. D. M. Wayner, P. Allongue and C. H. de Villeneuve, *J. Phys. Chem. B* **104**, 11157 (2000).
12. M. D. Porter, T. B. Bright, D. L. Allara and C. E. D. Chidsey, *J. Am. Chem. Soc.* **109**, 3559 (1987).
13. C. A. Widrig, C. Chung and M. D. Porter, *J. Electroanal. Chem.* **310**, 335 (1991).
14. B. Ewen, G. R. Strobl and D. Richter, *Faraday Discuss.* **19**, (1980).
15. H. Z. Yu, S. Morin, D. D. M. Wayner, P. Allongue and C. H. de Villeneuve, *J. Phys. Chem. B* **104**, 11157 (2000).
16. M. R. Linford, P. Fenter, P. M. Eisenberger and C. E. D. Chidsey, *J. Am. Chem. Soc.* **117**, 3145 (1995).
17. M. D. Porter, T. B. Bright, D. L. Allara and C. E. D. Chidsey, *J. Am. Chem. Soc.* **109**, 3559 (1987).
18. A. Ulman, J. E. Eilers and N. Tillman, *Langmuir* **5**, 1147 (1989).